Wavelets meet Burgulence : CVS-filtered Burgers equation

Romain Nguyen van yen,[1] Marie Farge,[1,*] Dmitry Kolomenskiy,[2] Kai Schneider,[2] and Nick Kingsbury[3]

[1] *LMD–CNRS, École Normale Supérieure, Paris, France*
[2] *MSNM–CNRS & CMI, Université de Provence, Marseille, France*
[3] *Department of Engineering, Cambridge University, U.K.*

(Dated: January 27, 2008)

Numerical experiments with the one dimensional inviscid Burgers equation show that filtering the solution at each time step in a way similar to CVS (Coherent Vortex Simulation) gives the solution of the viscous Burgers equation. The CVS filter used here is based on a complex-valued translation-invariant wavelet representation of the velocity, from which one selects the wavelet coefficients having modulus larger than a threshold whose value is iteratively estimated. The flow evolution is computed from either deterministic or random initial conditions, considering both white noise and Brownian motion.

PACS numbers: 47.27.Eq

I. INTRODUCTION

The fully developed turbulent regime is described by solutions of the Navier–Stokes equations for two or three-dimensional incompressible fluids, in the limit where the kinematic viscosity becomes very small. By analogy, Burgulence is described by the solutions of Burgers equations for a one–dimensional fluid in the same limit, as first proposed by Burgers [3] and advocated by von Neumann [19]. This toy model for turbulence has been extensively used since then [1, 13, 15, 21, 23]; Frisch and Bec have proposed to name it: *Burgulence* [11].

We consider the one-dimensional Burgers equation in a periodic domain of support $x \in [-1, 1]$, which describes the space–time evolution of the velocity $u(x, t)$ of a one–dimensional fluid flow :

$$\partial_t u + \frac{1}{2}\partial_x u^2 \;=\; \nu \partial_{xx} u \;, \qquad (1)$$

where ν denotes the kinematic viscosity. The solutions of (1) can be computed analytically using the Cole-Hopf transformation [4, 6, 14]. When $\nu \to 0$ the solutions of the viscous Burgers equation approach weak solutions of the inviscid problem. The uniqueness of these solutions stems from the condition that shocks have negative jumps, which guarantees energy dissipation. For Burgers equation, this condition is equivalent to an entropy condition [12, 17, 18, 20].

The wavelet representation has been proposed for studying turbulence [7], since it preserves both the spatial and spectral structures of the flow by realizing an optimal compromise in regard of the uncertainty principle. We have found that projecting the vorticity field onto a wavelet basis, and retaining only the strongest coefficients, extracts the coherent structures out of fully developed turbulent flows [8, 9]. We have then proposed a computational method for solving the Navier-Stokes equations in wavelet space [8]. We have shown that extracting the coherent contribution at each time step preserves the nonlinear dynamics, whatever its scale of activity, while discarding the incoherent contribution corresponding to turbulent dissipation [22]. This is the principle of the CVS (Coherent Vortex Simulation) method we have proposed [8, 10].

The aim of the present paper is to apply the CVS filter to the inviscid Burgers equation and check if this is equivalent to solving the viscous Burgers equation. The outline is the following. First we recall the principle of CVS filtering and its extension using complex-valued translation-invariant wavelets. The numerical scheme is described briefly and the main part presents results of several numerical experiments, considering either deterministic or random initial conditions. Finally, we draw conclusions and propose some perspectives.

II. NUMERICAL METHOD

The Burgers equation (1) is discretized on N grid points using a Fourier spectral collocation method :

$$\frac{\partial U}{\partial t} + \frac{1}{3} D_N(U^2) + \frac{1}{3} U \cdot D_N(U) - \nu D_N^2(U) = 0 \;, \qquad (2)$$

where U approximates $(u(x_0,t), u(x_1,t), ..., u(x_{N-1},t))$, D_N stands for the Fourier collocation differentiation and $\cdot$ is the pointwise product of two vectors. The discretization of the nonlinear term in (2) is chosen in order to conserve the kinetic energy $E = \frac{1}{2}\int_{-1}^{1} u^2(x,t)dx$ when $\nu = 0$ [5]. For time integration a fourth-order Runge-Kutta scheme is used.

At each time step, we will filter the solution using the CVS method which we now recall briefly. Given orthogonal wavelets (ψ_{ji}) and the associated scaling function at

*Electronic address: farge@lmd.ens.fr

the largest scale φ, the velocity can be expanded into :

$$u(x) = \langle u \mid \varphi \rangle \varphi(x) + \sum_{j=0}^{J-1} \sum_{i=1}^{2^j} \langle u \mid \psi_{ji} \rangle \psi_{ji}(x) \ , \qquad (3)$$

where j is the scale index, i is the position index and the inner product is $\langle a \mid b \rangle = \int_{-1}^{1} a(x) \cdot b^*(x) dx$ with b^* denoting the complex conjugate of b. Since location in orthogonal wavelet space is sampled on a dyadic grid, this representation breaks the local translation invariance of (1) which may impair the stability of the numerical scheme. Therefore we prefer using, instead of real-valued wavelets, complex valued wavelets [16] which very closely preserve translation invariance. In this case, (3) still holds as long as we replace the right hand side by its real part.

The CVS filter then consists in discarding the wavelet coefficients whose modulus is below a threshold T. In addition, wavelets coefficients at the finest scale are systematically filtered out. The resulting velocity u_T is a nonlinear approximation of u.

Because the velocity field decays in time, the threshold has to be estimated at each time step in a self-consistent way. To do this, we follow the iterative method introduced in [2], which consists in imposing the ratio between the standard deviation of the discarded wavelet coefficients and the threshold itself:

$$T^2 = \frac{5}{N_T} \sum_{j=0}^{J-1} \sum_{i=1}^{2^j} |\widetilde{u}_{ji}|^2 H(T - |\widetilde{u}_{ji}|) \ , \qquad (4)$$

where H is the Heaviside step function and N_T is the number of wavelet coefficient below the threshold. The solution of (4) is determined numerically using a fixed point iterative procedure [2], initialized with $T_0 = 5E/N$, where E is the total energy.

III. DETERMINISTIC INITIAL CONDITION

We consider Burgers equation (1) with the deterministic initial condition $u(t = 0, x) = -\sin(\pi x)$. We begin by comparing three computations: a Galerkin-truncated inviscid case ($\nu = 0$), a viscous case ($\nu = 10^{-4}$), and an inviscid case with the CVS filter applied at each time step. The solutions are computed up to time $t = 5$, using $N = 4096$ grid points.

By computing in the Galerkin-truncated inviscid case ($\nu = 0$), we check that our numerical scheme conserves energy (Fig. 1, left) as theoretically predicted. We observe that the final solution at $t = 5$ exhibits energy equipartition (Fig. 1, right) with a Gaussian velocity PDF, as expected. Notice that the the white line in Fig. 1 (right) corresponds to the wavelet energy spectrum, *i.e.*, the squared modulus of the wavelet coefficients computed with a complex-valued Morlet wavelet. It better exhibits the k^0 scaling, characteristic of the energy equipartition, than the highly oscillatory Fourier energy

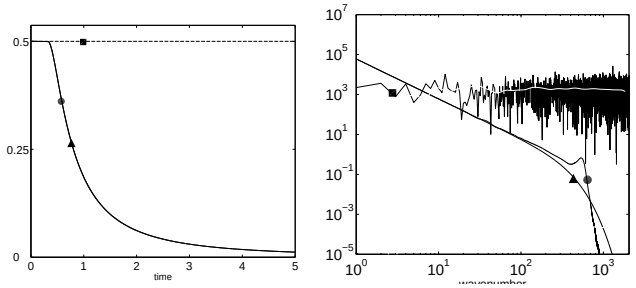

Figure 1: Deterministic initial conditions. Left: Time evolution of energy. Right: Energy spectrum at $t = 5$. We compare the Galerkin-truncated inviscid (square), viscous (triangle) and CVS-filtered inviscid (circle) cases. We observe that for the inviscid case (right) the wavelet spectrum (white line) better exhibits the energy equipartition than the Fourier spectrum (black line).

spectrum (black line). This illustrates the fact that the wavelet energy spectrum is more stable than the Fourier energy spectrum when we analyze only one realization of a stochastic process [7] and should rather be used in this case.

For the viscous and CVS-filtered inviscid cases, the energy remains basically constant until the shock forms at $t = 1/\pi$, but then decays with a t^{-2} law. In Fig. 1 (right) the energy spectra of the viscous and CVS-filtered inviscid cases exhibit a power law behaviour with slope -2.

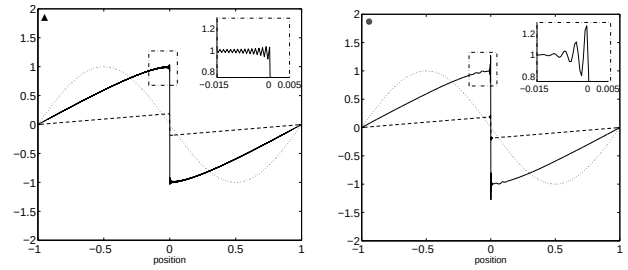

Figure 2: Deterministic initial conditions. Snapshots of velocity for the viscous (left) and the CVS-Filtered inviscid (right) cases at $t = 0$ (dotted line), $t = 0.5$ (solid line) and $t = 5$ (dashed line). The insets show the tip of the shock at $t = 0.5$.

Fig. 2 shows the velocity at three time instants for the viscous and CVS-filtered inviscid cases. The CVS-filtered inviscid solution yields the same dynamics as the viscous one and the only difference concerns the small overshoot we observe at $x = 0$ after the shock has formed. This Gibbs phenomenon is stronger but less oscillatory for the CVS-filtered inviscid case than for the viscous case (see the insets in Fig. 2).

The time evolution of the percentage of retained wavelet coefficients is presented in Fig. 3 (left). It shows that with only relatively few coefficients (about $7\%N$)

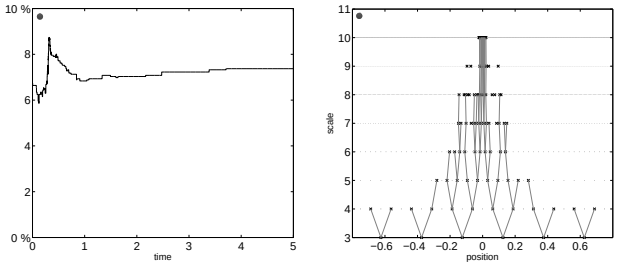

Figure 3: Deterministic initial conditions. Left: Time evolution of the percentage of wavelet coefficients retained after filtering. Right: Dyadic tree of the wavelet coefficients which are retained after filtering at $t = 5$. The crosses indicate the $7\%N$ retained wavelet coefficients, while the small dots correspond to the $93\%N$ discarded wavelet coefficients. The scale varies from coarse to fine, up the vertical axis.

we are able to track the nonlinear dynamics of the flow and this number remains almost constant after the shock formation. At $t = 5$, the retained wavelet coefficients are located around $x = 0$, the position of the shock, and span all scales there, as illustrated in Fig. 3 (right). About ten wavelet coefficients per scale are sufficient to represent the shock.

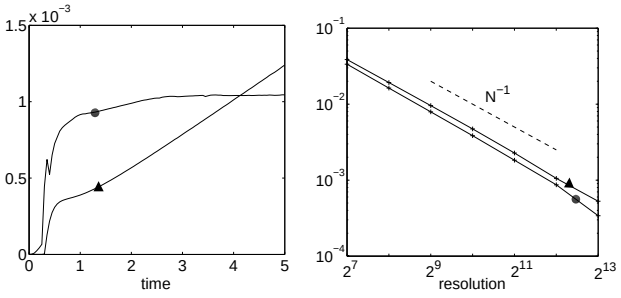

Figure 4: Deterministic initial conditions. Left: Time evolution of the relative mean squared error ϵ_N at $N = 4096$. Right: Relative mean squared error ϵ_N at $t = 5$ for different numerical resolutions, $N = 128$ to $N = 8192$. We compare the viscous (triangle) and CVS-filtered inviscid (circle) cases.

We now show that, when N increases, the filtered solutions converge towards the entropy solution $u_{\rm ref}$ which solves the Burgers equation in the inviscid limit. For comparison we also consider the viscous solutions with viscosity depending on N ($\nu = 0.4096N^{-1}$) which are known to converge to $u_{\rm ref}$ everywhere, except at $x = 0$. The entropy solution $u_{\rm ref}$ is directly calculated using the method of characteristics.

First, we consider a global error estimate, the relative mean square error, defined as:

$$\epsilon_N(t) = \frac{\|u - u_{\rm ref}\|_2^2}{\|u_{\rm ref}\|_2^2} \, . \tag{5}$$

On Fig. 4 (left) we plot $\epsilon_N(t)$ for $N = 4096$. The error for the CVS-filtered inviscid case is larger but saturates after $t \simeq 2$. In contrast, the error for the viscous case keeps increasing because the finite viscosity smooths the shock away. Considering now $t = 5$ and varying N, we find that for both the viscous and CVS-filtered inviscid cases ϵ_N decreases as N^{-1} (Fig. 4, right).

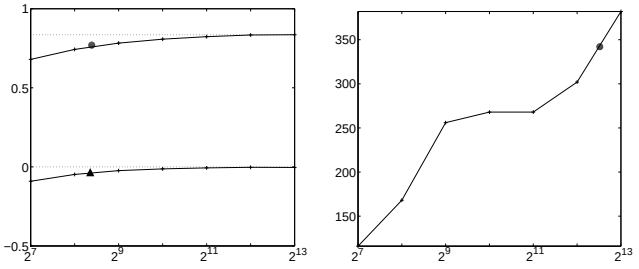

Figure 5: Deterministic initial conditions. Error on the relative total variation ϵ'_N (left), and number of retained wavelet coefficients (right), as functions of N at $t = 5$, for the viscous (triangle) and CVS-filtered inviscid (circle) solutions.

We now study the behaviour of the oscillations in the neighborhood of the shock when the resolution N is increased. The total variation of a function f on $[-1, 1]$ is defined by:

$$\|f\|_{TV} = \int_{-1}^{1} |\partial_x f| dx \, . \tag{6}$$

To detect the presence of spurious oscillations, we compute the relative error on the total variation:

$$\epsilon'_N(t) = \frac{\|u(x,t)\|_{TV} - \|u_{\rm ref}(x,t)\|_{TV}}{\|u_{\rm ref}(x,t)\|_{TV}} \, , \tag{7}$$

which is plotted as a function of N for $t = 5$ on Fig. 5 (left). For the viscous case, ϵ'_N is negative and converges towards zero when N increases. For the CVS-filtered inviscid case, ϵ'_N tends to a finite positive value close to 0.84. The overshoot that could be seen on Fig. 2 persists but becomes more and more localized around the singularity when N increases, thus ensuring that mean square convergence. Let us end this section by a short discussion on the evolution of the compression rate when N increases. Fig. 5 (right) shows that the number of retained wavelet coefficients increases roughly logarithmically as a function of N. As a consequence, notice that for the filtered solution, the relative mean square error $\epsilon_N(t)$, if it is considered as a function of the number of retained coefficients only, converges to zero exponentially fast. However, to experience this promising rate of convergence in practice, we should compute the evolution of u using only the wavelet coefficients whose modulus remains above the threshold.

IV. RANDOM INITIAL CONDITION

In the previous section we have demonstrated that the CVS-filtered inviscid Burgers equation exhibits an evolu-

tion similar to that of the viscous Burgers equation. We now would like to check if this is still verified in the context of *Burgulence* for both white noise [1] and Brownian motion [21].

a. White-noise initial condition We take as initial velocity one realization of a Gaussian white noise computed at resolution $N = 4096$, which corresponds to a random non intermittent initial condition. Since the CVS filter removes the non intermittent noisy contributions, if applied to a Gaussian white noise the latter would be completely filtered out. Therefore we first integrate the viscous equation with $\nu = 2 \cdot 10^{-5}$ without filtering, and wait until the flow intermittency has sufficiently developed before applying the filter. To check the flow intermittency we monitor the flatness of velocity gradient until it reaches the value 20, which happens at $t = 0.017$ for the realization described here. Then, we reset $t = 0$ and integrate up to $t = 5$, both the viscous equation with $\nu = 2 \cdot 10^{-5}$, and the CVS-filtered inviscid equation.

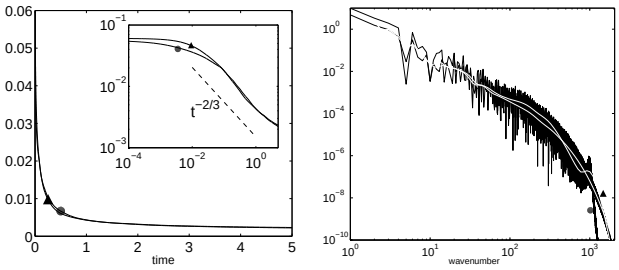

Figure 6: White noise initial conditions. Left: time evolution of energy. The inset shows the $t^{-2/3}$ decay in log-log coordinates. Right: energy spectrum at $t = 5$. We compare the viscous (triangle) and CVS-filtered inviscid (circle) simulations. We observe that the wavelet spectrum (white lines) better exhibits the k^{-2} scaling of energy than the Fourier spectrum (black lines).

In Fig. 6 (left) we show that the energy, for both the CVS-filtered inviscid solution and the viscous solution, decays with a $t^{-2/3}$ law, as found by Burgers [4, 21]. In Fig. 6 (right) we observe at $t = 5$ that both energy spectra present the same k^{-2} scaling. Notice that the two white lines in Fig. 6 (right) correspond to the wavelet energy spectrum, which better exhibit the k^{-2} scaling of the energy than the highly oscillatory Fourier energy spectrum (black lines).

Finally, we show on Fig. 7 that the viscous and CVS-filtered inviscid solutions are almost identical in physical space, presenting a typical sawtooth profile as first noticed by Burgers [4].

b. Brownian motion initial condition We use the same resolution $N = 4096$ as above, only the initial condition changes. Since we have chosen periodic boundary conditions we approximate the Brownian motion by the Fourier series:

$$u(x,0) = \sum_k u_k e^{ikx} \qquad (8)$$

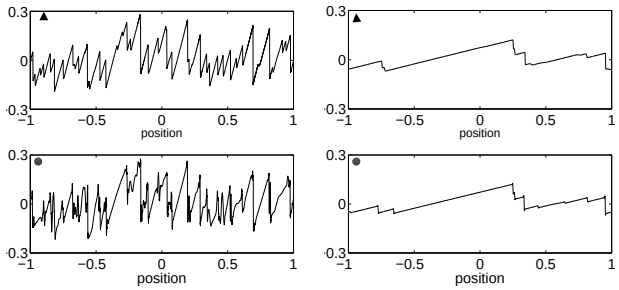

Figure 7: White noise initial conditions. Snapshots of velocity at $t = 0.3$ (left) and $t = 5$ (right). Top: viscous equation with $\nu = 2 \cdot 10^{-5}$ Bottom: CVS-filtered inviscid equation.

where $k = -\frac{N}{2} + 1, -\frac{N}{2}, ..., \frac{N}{2} - 1$. We set $u_0 = 0$ and, for $k \neq 0$, we take for u_k a complex Gaussian random variable with standard deviation $1/|k|$.

The solution for the viscous case is computed with $\nu = 1.2 \cdot 10^{-4}$. For the CVS-filtered inviscid case, as we did for the white noise initial condition, we do not filter before enough intermittency has developed. We thus integrate the viscous equation with $\nu = 1.2 \cdot 10^{-4}$ for 0.05 time units and then switch viscosity off. This procedure provides the initial velocity which by construction is the same for both methods (Fig. 8).

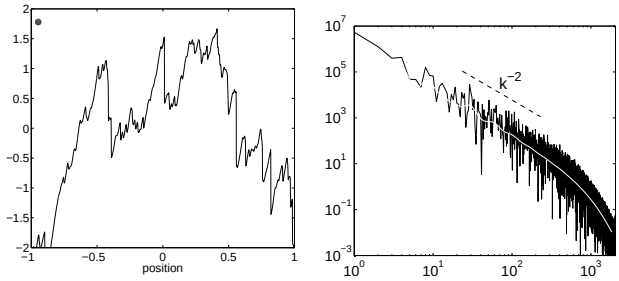

Figure 8: Brownian initial condition. Velocity at $t = 0$ (left) and its energy spectrum (right). We observe that the wavelet spectrum (white line) better exhibits the k^{-2} scaling of energy than the Fourier spectrum (black line).

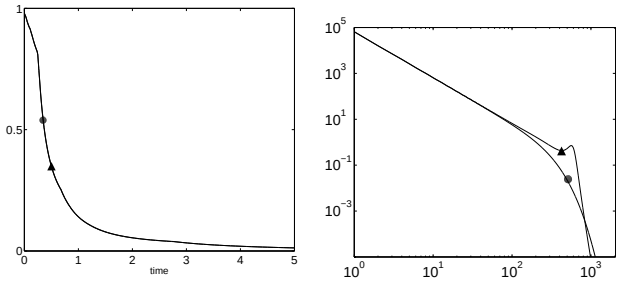

Figure 9: Brownian initial condition. Left: Time evolution of energy. Right: Energy spectrum at $t = 5$. We compare the viscous (triangle) and CVS-filtered inviscid (circle) cases.

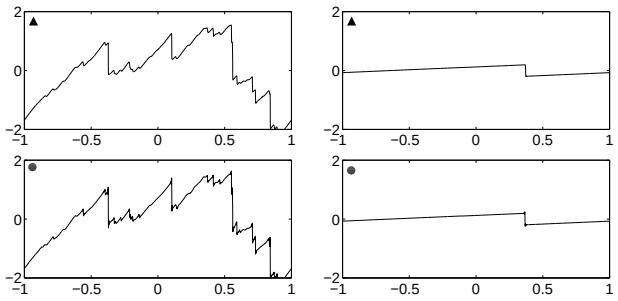

Figure 10: Brownian initial conditions. Snapshots of velocity at $t = 0.1$ (left) and $t = 5$ (right). Top: viscous equation with $\nu = 1.2 \cdot 10^{-4}$. Bottom :CVS-filtered inviscid equation.

The energy decay matches well between the CVS-filtered inviscid and the viscous solutions (Fig. 9, left). A k^{-2} power spectrum is also obtained for both at $t = 5$ (Fig. 9, right).

At $t = 0.1$ numerous small shocks are present on the viscous solution (Fig. 10, top left). All of them are correctly reproduced by the CVS-filtered inviscid solution (Fig. 10, bottom left).

At $t = 5$ the single remaining shock that is still resolved in the viscous solution (Fig. 10, top right) is correctly reproduced on the CVS-filtered inviscid solution (Fig. 10, bottom right).

V. CONCLUSION

We have shown that CVS-filtering at each time step the solution of the inviscid Burgers equation gives the same evolution as the viscous Burgers equation, for both deterministic and random initial conditions. As our contribution to Euler equations' 250th anniversary and Euler's 300th birthday, we conjecture that CVS-filtering of the Euler equation may be equivalent to solving the Navier–Stokes equations in the fully-developed turbulent regime, *i.e.*, when dissipation has become independent of viscosity. We predict that the retained wavelet coefficients would preserve Euler's nonlinear dynamics, while discarding the weaker wavelet coefficients would model turbulent dissipation and give Navier–Stokes solutions. Since in the fully-developed turbulent regime turbulent dissipation strongly dominates molecular dissipation, there is no reason to model turbulent dissipation by a Laplacian operator anymore. Indeed, turbulent dissipation is a property of the flow, while molecular dissipation is a property of the fluid and may no more play a role when turbulence is fully-developed. We think that in this regime the CVS filter could be a better way to model dissipation, replacing global by local smoothing while preserving nonlinear interactions. In this paper we have chosen the simplest toy model to test this conjecture, although Burgers' equation, in contrast to Euler's equation, is neither chaotic nor producive of randomness. Therefore we conjecture that the CVS-filter would work better for Euler/Navier–Stokes than for Burgers since CVS is based on denoising, which is justified when there is chaos and randomness.

Acknowledgments: We thank Uriel Frisch, Margarete Domingues, Claude Bardos, François Dubois and two anonymous referees for their useful comments. We acknowledge financial support from the ANR under contract M2TFP (Méthodes Multi-échelles pour la Turbulence Fluide et Plasma) and from the Association CEA-Euratom under contract V.3258.006. NK thanks the Universite de Provence for supporting his stay in Marseille. MF is grateful to the fellows of Trinity College, Cambridge (U.K.), in particular Keith Moffatt, for their kind hospitality while revising this paper.

[1] M. Avellaneda and W. E. *Commun. Math. Phys.*, **172**, 13-38, 1995.
[2] A. Azzalini, M. Farge and K. Schneider. *Appl. Comput. Harm. Anal.*, **18**(2), 177–185, 2005.
[3] J.M. Burgers. *Verh. KNAW, Afd. Natuurkunde, XVII*, **2**, 1-53, 1939.
[4] J.M. Burgers. *Proc. KNAW B, LVII*, **1**, 45-72, 1954.
[5] C. Canuto, M. Y. Hussaini, A. Quarteroni and T. A. Zang. *Spectral methods in fluid dynamics*. Springer-Verlag (1988).
[6] J. D. Cole. *Q. Appl. Math.*, **9**, 225, 1951.
[7] M. Farge. *Ann. Rev. of Fluid Mech.*, **24**, 395–457, 1992.
[8] M. Farge, K. Schneider and N. Kevlahan. *Phys. Fluids*, **11**(8), 2187–2201, 1999.
[9] M. Farge, G. Pellegrino and K. Schneider. *Phys. Rev. Lett.*, **87**(5), 45011–45014, 2001.
[10] M. Farge and K. Schneider. *Flow, Turbulence and Combustion*, **66**(4), 393–426, 2001.
[11] U. Frisch and J. Bec. *New trends in turbulence. Les Houches 2000, Vol. 74* (Eds. M. Lesieur, A. Yaglom and F. David), Springer, 341, 2002.
[12] P. Germain, R. Bader. *Note technique ONERA*, OA nø1/1711-1, May 1953.
[13] S. N. Gurbatov, S. I. Simdyankin, E. Aurell, U. Frisch and G. Tóth. *J. Fluid Mech.*, **344**, 339–374, 1997.
[14] E. Hopf. *Comm. Pure Appl. Math.*, **3**, 201, 1950.
[15] S. Kida. *J. Fluid Mech.*, **79**, 337–377, 1997.
[16] N. Kingsbury. *Appl. Comput. Harm. Anal.*, **10** (3), 234–253, 2001.
[17] S. N. Kruzhkov. *Math. USSR Sb.* , **10**, 2, 217-243, 1970. (*Amer. Math. Transl.*, Series 2, **26**, 95-172)
[18] P.-D. Lax. *Comm. Pure Appl. Math.*, **7**, 159-193, 1954.
[19] J. von Neumann. *Collected works*, ed. A.H. Taub, **5**, Pergamon, 437-471, 1961.
[20] O. Oleinik. *Usp. Mat. Nauk*, **12**, 3, 3-73, 1957. (*Amer. Math. Transl.*, Series 2, **26**, 95-172)
[21] Z. S. She, E. Aurell and U. Frisch *Commun. Math. Phys.*, **148**, 623-641, 1992.

[22] K. Schneider, M. Farge, G. Pellegrino, and M. Rogers. *J. Fluid Mech.*, **534**, 39–66, 2005.
[23] M. Vergassola, B. Dubrulle, U. Frisch, and A. Noullez. *Astron. Astrophys.*, **289**, 325–356, 1994.